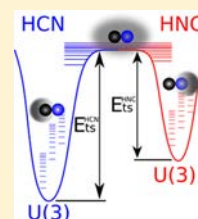


Calculation of Transition State Energies in the HCN–HNC Isomerization with an Algebraic Model

Jamil Khalouf-Rivera,[†] Miguel Carvajal,^{†,§} Lea F. Santos,[‡] and Francisco Pérez-Bernal^{*,†,§}[†]Depto. de Ciencias Integradas y Centro de Estudios Avanzados en Física, Matemáticas y Computación, Universidad de Huelva, Huelva 21071, Spain[‡]Department of Physics, Yeshiva University, New York, New York 10016, United States[§]Instituto Carlos I de Física Teórica y Computacional, Universidad de Granada, Granada 18071, Spain

Supporting Information

ABSTRACT: Recent works have shown that the spectroscopic access to highly excited states provides enough information to characterize transition states in isomerization reactions. Here, we show that information about the transition state of the bond-breaking HCN–HNC isomerization reaction can also be achieved with the two-dimensional limit of the algebraic vibron model. We describe the system's bending vibration with the algebraic Hamiltonian and use its classical limit to characterize the transition state. Using either the coherent state formalism or a recently proposed approach by Baraban et al. [*Science* 2015, 350, 1338–1342], we obtain an accurate description of the isomerization transition state. In addition, we show that the energy-level dynamics and the transition state wave function structure indicate that the spectrum in the vicinity of the isomerization saddle point can be understood in terms of the formalism for excited-state quantum phase transitions.



1. INTRODUCTION

Transition state theory is the keystone of chemical reaction studies and chemical kinetics since its formulation in the 1930s.^{1,2} It allows for the derivation of thermal reaction rates from the energy surface landscape, in particular, from the minimal energy pathway connecting reactants and products. However, the experimental study of transition states is hindered by the saddle structure of the phase-space region they inhabit. In recent works, Baraban et al.³ and Mellau et al.⁴ presented an interesting approach that allows for the characterization of the transition state in isomerization reactions using spectroscopic data in the frequency domain as an input. The approach in both works is based on a particular spectroscopic pattern: the appearance of a dip in the spacing of adjacent quantum levels for overtone series associated with degrees of freedom that are connected with the reaction coordinate.

In molecular spectroscopy, the increase in the level density, which happens together with the decrease in the energy difference between neighboring energy levels, indicates that the system is reaching a region subject to significant changes in its potential shape. An example is the well-known energy-level piling up that occurs once a system gets close to dissociation. Birge and Sponer were already aware of the importance of effective frequency⁵ and the Birge–Sponer plots, of great relevance in the study of molecular dissociation and in the estimation of dissociation energies, reflect the decrease in the effective frequency value once the system excitation energy approaches the dissociation energy. The deviation from linearity in Birge–Sponer plots can be explained from the potential shape and it may be parameterized to obtain a very precise estimation of the system dissociation energy.^{6,7}

Nonrigid molecular systems also experience an increase in the energy-level density when the system explores the top of the barrier to linearity. In this case, the adjacent quantum-level splittings pass through a minimum value, where anharmonicity switches from negative to positive values. This feature is known as the Dixon dip since the seminal work of Dixon, who showed that the vibrational bending degrees of freedom of a quasilinear molecule can be modeled with a cylindrically symmetric potential with a hump in the origin.⁸ He evinced the cusp in the effective frequency at the energy of the barrier to linearity. This has been later explained with the concept of quantum monodromy, which elucidates the spectral features associated with the qualitative change in the system phase-space configuration that happens once the system energy reaches the local potential maximum, at the top of the barrier to linearity.^{9–11}

The formalism presented in ref 3 relates the dip in the quantum level spacing in isomerizing systems with the saddle (or local maximum) structure of the potential at energies around the isomerization barrier height. The work proposed a simple phenomenological formula to extract the isomerization barrier height from spectroscopic data. This formula was applied to the vibrational bending spectrum of two isomerizing systems that have been subject to extensive theoretical and experimental analyses: the HCN–HNC bond-breaking system and the cis–trans configurations in the acetylene S_1 electronic state. In both cases, it was shown how the proposed method helps to identify isomerization pathways, allowing for the

Received: August 1, 2019

Revised: October 8, 2019

Published: October 9, 2019

distinction between spectator vibrational modes and those particular combinations of modes that favor the isomerization reaction path. They were also able to extract the transition state energies, E_{TS} , well within 1% of the value of the isomerization barrier height obtained with sophisticated ab initio calculations.^{12–15}

Therefore, both isomerizing and nonrigid molecular species may be described from a common perspective. In the first case, the critical point is associated with the transition state saddle point,^{3,4} while in the second case, it is connected with the top of the barrier to linearity.^{16–18} The questions addressed here are whether an algebraic model like the two-dimensional limit of the vibron model (2DVM) can be of help in the estimation of the transition state properties from spectroscopic data and if the decrease in the separation between energy levels can be considered as a new example of excited-state quantum phase transition (ESQPT).

We show that the 2DVM, once furnished with enough spectroscopic information, can also be used to characterize the transition state with great accuracy. The 2DVM stems from the vibron model introduced by Iachello in the 1980s, an algebraic model for molecular structure that treats rovibrational excitations as bosonic particles (vibrons) with a $U(4)$ dynamical algebra (or spectrum-generating algebra).^{19,20} The 2DVM is tailored for the treatment of bending dynamics with a $U(3)$ dynamical algebra.²¹ Despite its apparent simplicity, the 2DVM encompasses in a common framework the two limiting cases of interest in the case of bending vibrations; rigidly linear and rigidly bent configurations, as well as the feature-rich nonrigid case, with particular spectroscopic signatures due to the existence of a barrier to linearity.^{22,23} The classical (or mean-field) limit of the 2DVM can be obtained with the coherent (or intrinsic) state formalism,^{24,25} which provides an exact energy functional in the large system size limit.²⁶

We perform calculations for the HCN–HNC system defining an algebraic Hamiltonian and, to get close enough to the isomerization barrier, we perform a fit to spectroscopically assigned ab initio term values,¹² as in ref 3. The assignment of these levels to the right quantum labels was performed in refs 13, 14 and implied an exhaustive analysis of the full experimental rovibrational spectrum for the [H, C, N] system. From the results of this fit, we estimate the isomerization barrier energy in two ways. First, we obtain the energy functional associated with the optimized algebraic Hamiltonian for both molecules making use of the coherent state formalism. From the potential shape, we estimate the value of the transition state energy. Next, we apply the phenomenological formula put forward by Baraban et al.³ to the term values predicted by the optimized algebraic Hamiltonian, obtaining a second estimation of the saddle point energy. Moreover, we explore how the structure of the wave function is affected once the system reaches energies around the isomerization barrier and we relate this change to the occurrence of an ESQPT in isomerizing systems.

The present work is organized as follows: Section 2 gives a brief introduction to the 2DVM algebraic formalism and on how to obtain its classical limit making use of the intrinsic (coherent) state formalism. Section 3 presents and explains the results. Section 4 contains our concluding remarks.

2. THEORY

The modeling of n -dimensional many-body systems using a $U(n + 1)$ spectrum-generating algebra provides an effective

description of a large variety of systems.²⁷ The most successful examples of this approach, undoubtedly, are the interacting boson model in nuclear physics and the vibron model in molecular physics. The first one is based on a $U(6)$ Lie algebra as its dynamical algebra²⁸ and the second one relies on a $U(4)$ Lie algebra.²⁰ In the present section, we briefly outline the theoretical basis of the 2DVM.

The 2DVM was initially presented by Iachello and Oss for the study of single and coupled benders.²¹ The model was found capable of reproducing the characteristic spectroscopic features that plague the bending spectrum of nonrigid molecular species.^{22,23} Despite its apparent simplicity, the model includes both a ground-state and an excited-state quantum phase transition. By conveniently parameterizing the 2DVM Hamiltonian, the system ground state can be made to evolve from a rigidly linear to a rigidly bent configuration through the variation of a control parameter. In this process, the ground state undergoes a particularly abrupt change at a critical value of the control parameter. This sudden change has been interpreted as a quantum phase transition,²⁶ a zero-temperature phase transition purely due to quantum fluctuations, in the same fashion as in other many-body bosonic systems.^{29–31} ESQPTs, defined later,^{32,33} generalize this concept to encompass excited states and are characterized by a singularity (in the mean-field limit) in the system density of states at a critical energy value. This singularity defines a separatrix between states having different characteristics.^{32,33} Precursors of ESQPTs have been identified in the vibrational bending spectra of several molecular species and have been associated, through the intrinsic state formalism, with the existence of a barrier to linearity in the energy potential.^{17,18} The singularity in the spectrum, marked by a pronounced decrease in level distance, happens once the system energy approaches the top of the barrier. The particular spectroscopic features that appear at such energies were explained by introducing the concept of quantum monodromy.^{9,10} The development of new spectroscopy techniques has made it possible to access experimentally excited vibrational states at energies beyond the barrier to linearity.^{34,35} Quantum monodromy can be interpreted as an ESQPT in the 2DVM,^{26,33} and the spectral signatures found in the vibrational bending spectra of some nonrigid molecular species have been considered the first experimental confirmation of the occurrence of an ESQPT.^{17,18} Other experimental systems where ESQPT signatures have been identified are superconducting microwave billiards³⁶ and spinor Bose–Einstein condensates.³⁷

2.1. Algebraic Approach to Bending Vibrations. The algebraic approach to bending vibrations is based on a bosonic $U(3)$ Lie algebra due to the inherently 2D nature of bending vibrations. The building bricks for this two-level boson model are a scalar boson, σ^\dagger , and two degenerate Cartesian bosons $\{\tau_x^\dagger, \tau_y^\dagger\}$. The nonzero commutation relations between creation and annihilation operators are

$$[\sigma, \sigma^\dagger] = 1, \quad [\tau_i, \tau_j^\dagger] = \delta_{i,j}; \quad i, j = x, y \quad (1)$$

All other commutators are zero. It is convenient to transform Cartesian into circular bosons²⁶

$$\tau_\pm^\dagger = \mp \frac{\tau_x^\dagger \pm i\tau_y^\dagger}{\sqrt{2}}, \quad \tau_\pm = \mp \frac{\tau_x \mp i\tau_y}{\sqrt{2}} \quad (2)$$

The nine $U(3)$ Lie algebra generators are the bilinear products of a creation and an annihilation operator. For a better physical insight, they are expressed as^{21,27}

$$\begin{aligned}\hat{n} &= \tau_+^\dagger \tau_+ + \tau_-^\dagger \tau_-, & \hat{n}_s &= \sigma^\dagger \sigma, & \hat{l} &= \tau_+^\dagger \tau_+ - \tau_-^\dagger \tau_-, \\ \hat{D}_\pm &= \sqrt{2} (\pm \tau_\pm^\dagger \sigma \mp \sigma^\dagger \tau_\pm), & \hat{Q}_\pm &= \sqrt{2} \tau_\pm^\dagger \tau_\mp, \\ \hat{R}_\pm &= \sqrt{2} (\tau_\pm^\dagger \sigma + \sigma^\dagger \tau_\mp)\end{aligned}\quad (3)$$

The next step in the algebraic procedure is to consider the possible dynamical symmetries, subalgebra chains starting in the dynamical algebra and ending in the system's symmetry algebra. In the present case, the system is limited to a plane and 2D angular momentum (vibrational angular momentum in molecular bending vibrations) is conserved; thus, the symmetry algebra is the $SO(2)$ Lie algebra. The generator of $SO(2)$ is the vibrational angular momentum, \hat{l} , as one can easily understand once it is expressed in terms of the Cartesian boson operators. As this is an angular momentum projection in the direction perpendicular to the system's plane, it can take both positive and negative (or zero) values. There are two possible dynamical symmetries that start in $U(3)$ and end in $SO(2)$

$$U(3) \supset U(2) \supset SO(2) \text{ Chain I} \quad (4a)$$

$$U(3) \supset SO(3) \supset SO(2) \text{ Chain II} \quad (4b)$$

Each dynamical symmetry conveys a basis and an analytical energy formula that can be associated with a physical limiting case. The $U(2)$ dynamical symmetry, also called the cylindrical oscillator symmetry, corresponds to a rigidly linear molecule, while the $SO(3)$ dynamical symmetry is associated with a rigidly bent configuration. A detailed discussion of both dynamical symmetries, their geometric implications, and the relation between them can be found in ref 26. All calculations in the present work have been performed using the chain I basis, the cylindrical oscillator basis, whose states are denoted as $|[N]; n'\rangle$. The quantum number N labels the totally symmetric representation of $U(3)$ and it is related to the total number of bound states of the system. Being a constant, hereafter, we simplify the basis states notation to $|n'\rangle$. The quantum label n indicates the vibrational number of quanta and l is the vibrational angular momentum. The branching rules are

$$\begin{aligned}n &= N, N-1, N-2, \dots, 0 \\ l &= \pm n, \pm(n-2), \dots, \pm 1 \text{ or } 0, (n = \text{odd or even})\end{aligned}\quad (5)$$

The definition of a simple Hamiltonian that contains the main physical ingredients of the model and allows for the study of the shape phase transition between the different dynamical symmetries implies the consideration of Casimir or invariant operators of the subalgebra chains under study.^{24,25} A simple model Hamiltonian includes the first-order Casimir operator of $U(2)$, \hat{n} , and the second-order Casimir operator of $SO(3)$, $\hat{W}^2 = (\hat{D}_+ \hat{D}_- + \hat{D}_- \hat{D}_+)/2 + \hat{l}^2$.

To reproduce the bending spectrum of HCN and HNC, we use the algebraic Hamiltonian

$$\hat{H} = P_{11} \hat{n} + P_{21} \hat{n}^2 + P_{22} \hat{l}^2 + P_{23} \hat{W}^2 + P_{45} [\hat{W}^2 \hat{n}^2 + \hat{n}^2 \hat{W}^2] \quad (6)$$

extending the most general one- and two-body Hamiltonian, employed in ref 18, with a four-body operator. The parameter

P_{ij} comes with the j th i -body operator in the Hamiltonian. The matrix elements of the one- and two-body operators in chain I basis are

$$\langle n' | \hat{n} | n' \rangle = n, \quad \langle n' | \hat{n}^2 | n' \rangle = n^2, \quad \langle n' | \hat{l}^2 | n' \rangle = l^2 \quad (7)$$

$$\begin{aligned}\langle n_2' | \hat{W}^2 | n_1' \rangle &= \\ &= -\sqrt{(N-n_1+2)(N-n_1+1)(n_1+l)(n_1-l)} \delta_{n_2, n_1-2} \\ &+ [(N-n_1)(n_1+2) + (N-n_1+1)n_1 + l^2] \delta_{n_2, n_1} \\ &- \sqrt{(N-n_1)(N-n_1-1)(n_1+l+2)(n_1-l+2)} \delta_{n_2, n_1+2}\end{aligned}\quad (8)$$

The four-body operator $[\hat{W}^2 \hat{n}^2 + \hat{n}^2 \hat{W}^2]$ is used here exclusively to improve the HCN data fit, and its matrix elements are

$$\begin{aligned}\langle n_2' | \hat{n}^2 \hat{W}^2 + \hat{W}^2 \hat{n}^2 | n_1' \rangle &= \\ &= -[n_1^2 + (n_1-2)^2] \sqrt{(N-n_1+2)(N-n_1+1)(n_1+l)(n_1-l)} \delta_{n_2, n_1-2} \\ &+ 2n_1^2 [(N-n_1)(n_1+2) + (N-n_1+1)n_1 + l^2] \delta_{n_2, n_1} \\ &- [n_1^2 + (n_1+2)^2] \sqrt{(N-n_1)(N-n_1-1)(n_1+l+2)(n_1-l+2)} \delta_{n_2, n_1+2}\end{aligned}\quad (9)$$

Operators \hat{n} , \hat{n}^2 , and \hat{l}^2 are diagonal in the $U(2)$ basis and can be identified with a harmonic term, an anharmonic correction, and the vibrational angular momentum, respectively. By contrast, the operator \hat{W}^2 is diagonal in the chain II basis and it is associated with an anharmonic displaced oscillator. The four-body operator combines Casimir operators from both subalgebra chains and it is not diagonal in any of them. Using the procedure sketched in the next section, we obtain a set of optimized spectroscopic parameters P_{ij} for each molecule.

2.2. Classical Limit of the Two-Dimensional Vibron Model. A system energy functional can be retrieved from the algebraic Hamiltonian (eq 6) by the method of coherent (intrinsic) states originally introduced in the study of nuclei,^{24,25,38,39} and later adapted to molecular systems.⁴⁰ There are other methods to establish a link between the phase space and the algebraic approaches.⁴¹

The intrinsic state method defines a coherent state, where the variational parameters r and θ are, in general, complex and represent coordinates and momenta.⁴⁰ We consider the spatial dependence only and, therefore, we set the momenta equal to zero.²⁰ We now proceed to outline the more relevant results needed to obtain the classical limit of the 2DVM. For a detailed description of this procedure in the 2DVM case, see refs 17, 18, 26.

The first step is the coherent state definition

$$|c.s.\rangle \equiv |[N]; r, \theta\rangle = \frac{1}{\sqrt{N!}} (b_c^\dagger)^N |0\rangle \quad (10)$$

where r and θ are the polar coordinates associated with Cartesian coordinates x and y . The operator b_c^\dagger is the boson condensate creation operator, $b_c^\dagger = \frac{1}{\sqrt{1+r^2}} [\sigma^\dagger + (x\tau_x^\dagger + y\tau_y^\dagger)]$.

The expectation value of the Hamiltonian (eq 6) in the coherent state gives as a result the ground-state energy functional, $E(r)$, akin to the system potential function

Table 1. Optimized Spectroscopic Parameters P_{ij} (cm^{-1} units), Root Mean Square Deviation rms (cm^{-1}), and Vibron Number N Obtained from the Fit to the HCN and HNC Ab Initio Data Set^{12,14,45} for Hamiltonian (eq 6)^a

| molecule | P_{11} | P_{21} | P_{22} | P_{23} | $P_{45} \times 10^4$ | N | rms |
|----------|-------------|-------------|------------|------------|----------------------|-----|-------|
| HCN | 2308.3(6) | -39.947(14) | 21.810(6) | -10.635(3) | -1.311(3) | 50 | 19.37 |
| HNC | 1024.9(1.4) | -18.59(4) | 13.362(23) | -5.085(11) | | 40 | 14.91 |

^aFor a detailed description of the fitting procedure, see the [Supplementary Material](#).

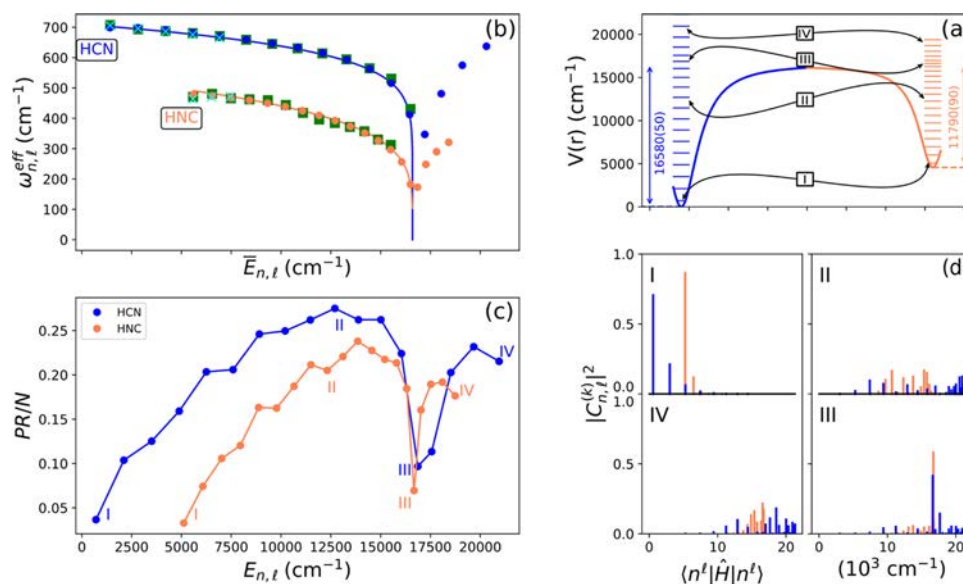


Figure 1. (a) Sketch of the potentials obtained for the two molecular species using the intrinsic state formalism and the isomerization barrier values, locating states I, II, III, and IV chosen to illustrate our results (see text). (b) Effective frequency $\omega_{n,l}^{\text{eff}}$ as a function of the midpoint excitation energy \bar{E} for HCN and HNC. Crosses indicate the available experimental data, while green squares are spectroscopically assigned ab initio results (ref 12, see text). Blue (orange) circles are the algebraic model results and the blue (orange) line marks the result of fitting eq 12 to the algebraic fit results for HCN (HNC). (c) Normalized participation ratio (see eq 13) of $l = 0$ HCN (blue dots) and HNC (orange dots) eigenstates resulting from the fit of the algebraic Hamiltonian (eq 6) (see [Supplementary Material](#) for details) making use of a truncated cylindrical oscillator basis. (d) Squared components in the cylindrical oscillator basis for four algebraic model eigenstates of HCN (blue bars) and HNC (orange bars) as a function of the expectation value of the Hamiltonian in the $|n^l\rangle$ basis state.

Table 2. Isomerization Barrier Height in cm^{-1} Units for HCN and HNC Computed from the Bending Energy Functional (2DVM-I) and from the 2DVM Optimized Term Values Using eq 12 (2DVM-II) Compared with Results Obtained Using Other Approaches (Columns Third to Fifth)

| molecule | E_{TS} comparison (cm^{-1}) | | | | |
|-----------------|---|------------|-----------------------------|-----------------------------|------------------------------|
| | 2DVM-I | 2DVM-II | Baraban et al. ³ | Mourik et al. ⁴⁵ | Makhnev et al. ⁴⁶ |
| HCN ($l = 0$) | 16 580(50) | 16 599(15) | 16 695(17) | 16 798 | 16 809.4 |
| HNC ($l = 0$) | 11 790(90) | 11 977(15) | 11 533(124) | 11 517 | 11 496.6 |

$$\begin{aligned}
 E(r) &= \frac{\langle \text{c. s.} | \hat{H} | \text{c. s.} \rangle}{N} = P_{11} \frac{r^2}{1+r^2} + \\
 &P_{21} \left[\frac{r^2}{1+r^2} + (N-1) \frac{r^4}{(1+r^2)^2} \right] + P_{22} \frac{r^2}{1+r^2} + \\
 &P_{23} \left[2 + (N-1) \frac{4r^2}{(1+r^2)^2} \right] + P_{45} \left[4 \frac{r^2}{1+r^2} + (N-1) \frac{12r^4 + 16r^2}{(1+r^2)^2} \right. \\
 &\left. + (N-1)(N-2) \frac{4r^6 + 28r^4}{(1+r^2)^3} + (N-1)(N-2)(N-3) \frac{8r^6}{(1+r^2)^4} \right] \quad (11)
 \end{aligned}$$

The equilibrium configuration of the molecule is obtained by minimizing $E(r)$ with respect to the variable r .

3. RESULTS AND DISCUSSION

To shed light on the estimation of the transition state properties and the possible link between isomerization and ESQPTs, we analyze the available data for the HCN–HNC

system. The available experimental data for the bending vibrational spectrum of HNC and HCN were already successfully modeled with a four-parameter 2DVM spectroscopic Hamiltonian, which is the most general Hamiltonian including one- and two-body interactions.¹⁸ Unfortunately, experimental data are not available above 10 000 cm^{-1} and the dissociation barrier is expected to lie around 17 000 cm^{-1} above the HCN minimum, which is located approximately 5200 cm^{-1} below the HNC minimum. To overcome this obstacle, we adopt the same approach as in Baraban et al.:³ we use for our calculations a set of ab initio term values¹² spectroscopically assigned after an exhaustive analysis of the full experimental rovibrational spectrum for the [H, C, N] system.^{13,14} In the present work, selecting pure bending levels, we consider 142 energies with vibrational angular momenta up to $l = 12$ in the case of HCN compared to 30 available experimental terms and 41 energy levels up to $l = 9$ in the case

of HNC compared to only 19 experimental levels. The optimization of the spectroscopic parameters was carried out through an iterative nonlinear least-square fitting procedure that uses the Fortran version of `Minuit`⁴² and the optimal values computed are included in Table 1 (see Supplementary text for details of the fits).

Once we optimize the spectroscopic parameter values in the algebraic Hamiltonian (eq 6), we compute the vibrational bending energy functional for both HCN and HNC using eq 11 derived from the intrinsic state formalism. The obtained functionals, depicted in Figure 1a, allow for the estimation of the isomerization barrier height, E_{TS} , which corresponds to the distance between the functional minimum and its asymptotic value. We provide in the column labeled 2DVM-I of Table 2 the obtained E_{TS} values for HCN and HNC.

Baraban et al. calculate the transition state energy with a different approach. They quantify the observed energy dip making use of the effective frequency, a quantity defined for quantum systems as $w^{\text{eff}}(n) = \frac{\partial E(n)}{\partial n} = \frac{\Delta E}{\Delta n}$, i.e., the discrete derivative of the system energy with respect to the principal quantum number n .^{3,4} They suggest a simple formula³ to parameterize the dependence of the effective frequency on the midpoint vibrational energy \bar{E} ,

$$w^{\text{eff}}(\bar{E}) = \omega_0 \left(1 - \frac{\bar{E}}{E_{\text{TS}}} \right)^{1/m} \quad (12)$$

with three adjustable parameters: ω_0 , m , and E_{TS} . The parameter ω_0 is the effective frequency for the potential ground state and m depends on the potential shape.³ The most relevant parameter is E_{TS} , the transition state energy, which provides an estimate of the energy barrier between different reactants.

We derive the transition state energy employing an alternative procedure. We use the effective frequencies computed from the term values predicted using the 2DVM for both molecular species. The results for $l = 0$ vibrational angular momentum are shown in Figure 1b, where ω^{eff} is plotted as a function of \bar{E} using blue (orange) circles for the algebraic model results for HCN (HNC). The effective frequency for spectroscopically assigned ab initio data is depicted using green squares and the available experimental data are also included as (cyan) crosses. It is clear from this figure that the 2DVM results undergo the expected dip in the effective frequency and that they provide a very good estimate of the height of the isomerization barrier in the HCN–HNC molecular system. The HNC data are displaced so that the top of the barrier is common for both molecular species, which allows for the estimation of the separation between the HCN and HNC energy minima. We use the effective frequency of the algebraic term values to fit the parameters in the function (eq 12) with the help of the Python `LMFIT` package,⁴³ and obtain the estimated barrier values in the column of Table 2 labeled as 2DVM-II.

The agreement between the values of the transition state energy obtained with the two methods above and the values obtained with other approaches is very good, as can be seen in Table 2. The differences of the E_{TS} value with respect to sophisticated ab initio calculations are 1–2% in the HCN case, and they increase to a maximum of 4% in the HNC case. The explanation for this difference lies in the fact that the HNC bending potential has an unusual shape from the interaction

with a nearby excited diabatic electronic state.⁴⁴ To overcome this obstacle, Baraban et al.³ included a Gaussian term into their phenomenological formula (eq 12). The lack of this extension in the present work explains the different agreement with the results obtained using other approaches for HCN and HNC.

An advantage of the algebraic model, compared to a pure Dunham expansion, is that it provides not only the spectrum but also the eigenstates of Hamiltonian (eq 6) upon diagonalization. The height of the isomerization barrier has strong consequences for the structure of the eigenstates and the dynamics of the HCN–HNC molecular system.^{47–49} Indeed, it has been recently shown that the system's eigenstate with the closest energy to the saddle point that characterizes the transition state has an enhanced localization in the bending coordinates.⁴ A similar phenomenon has been discussed in the case of ESQPTs in different realizations of the vibron model, where eigenstates with eigenvalues close to the critical energy of the ESQPT have been shown to be strongly localized in the basis associated with the linear configuration, also called the cylindrical oscillator basis.^{50–52}

The level of localization of states written in a certain basis can be quantified with quantities such as the information (or Shannon) entropy or the participation ratio (PR).^{53,54} A large PR value implies that the state receives significant contributions from many basis states and a small PR value denotes a strong localization of the state in the basis. This is similar to other quantities, such as Heller's F parameter, used to probe phase-space flow in molecular systems.^{55,56} Hamiltonian (eq 6) is block-diagonal in the vibrational angular momentum l . Its eigenstates can be written as a linear combination of the cylindrical oscillator basis states $\{|[N]n^l\rangle\}; |\psi_k^{(l)}\rangle = \sum_n C_{k,n}^l |n^l\rangle$ and the participation ratio is defined as

$$\text{PR}(|\psi_k^{(l)}\rangle) = \left[\sum_n |C_{k,n}^l|^4 \right]^{-1} \quad (13)$$

The minimum PR value is 1, when the system localization is maximal and the eigenstate can be identified with a basis state. The maximum PR value is the dimension of an l -vibrational angular momentum basis block, which happens when all components are nonzero and have the same weight.

In the nonrigid case, the eigenstate at the ESQPT critical energy is strongly localized in the chain I basis state with $n = 0$. This has been shown to affect the system dynamics. If the system is initially prepared in this initial basis state, the evolution is substantially slower than that for other initial states with similar energy.^{50–52,57} Similarly, the eigenstate at the isomerization barrier is also localized, but with a caveat, as we explain next. In the HCN–HNC case, we plot the PR for the $l = 0$ eigenstates normalized by the vibron number N in Figure 1c with blue (orange) dots for HCN (HNC). In both cases, there is a remarkable decrease in the PR value for eigenstates close to the isomerization energy value. To further clarify the variation in the eigenstates structure, we include in Figure 1a the two energy functional curves and the energies of four eigenstates chosen to illustrate the different structures of the wave functions at different excitation energies. These states are also indicated in Figure 1c. The four selected eigenstates of HCN and HNC, labeled as I, II, III, and IV, have energies at different locations in the potential: at the ground-state energy, at a mid-height, at the isomerization barrier, and above the

barrier. The bar diagrams in the four panels of Figure 1d are drawn from the squared value of the $C_{k,n}^l$ coefficients for those four eigenstates as a function of the energy of the corresponding basis vector, $\langle Nn'|\hat{H}|Nn'\rangle$; bars are blue (orange) for HCN (HNC) eigenstates. The change in the structure as we move from eigenstate I to IV is evident. The low-energy eigenstate I is localized because the cylindrical oscillator basis is the most appropriate basis for the description of rigidly linear configurations. Eigenstates II and IV are characterized by a strong mixing in the same basis. Eigenstate III is of special relevance since it is the eigenstate with the closest energy to the isomerization barrier. It is characterized by a strong localization in the cylindrical oscillator basis. Contrary to what happens in the ESQPT for nonrigid molecules, where for $l = 0$ the basis element $|N0^0\rangle$ has the largest component,^{50–52} in the isomerization case, the minimum in the PR is associated with a large component in a basis state with a high n value, e.g., $|NN^0\rangle$ for an even N value. This is likely caused by anharmonicity effects in the Hamiltonian, as already hinted in ref 58. Indeed, we verified that a negative quadratic contribution in the vibrational quantum number operator has effects in the symmetric phase for linear and quasilinear states before the control parameter reaches the critical value.

4. CONCLUSIONS

In short, we have shown that the 2DVM, despite the simplicity of the Hamiltonian (eq 6), describes extremely well the localization and the effective frequency dip of the transition state for isomerizing systems, once it is fed with enough spectroscopic data or with accurate enough ab initio calculations. The value of the transition state energy can be estimated from the intrinsic state energy functional or from the dip in the energy gap. In both cases, the differences with the E_{TS} values obtained with sophisticated ab initio calculations are very small, in the range 1–4%. As a consequence of the link between the isomerization barrier and ESQPTs, our characterization of the transition state is not restricted to energy values and their differences only, but includes also the structure of the algebraic wave function. This offers a promising line of research for applications of the ESQPT formalism to isomerization reactions.

Our approach also provides a physically sound way for obtaining a minimum bound for the vibron number value N , which needs to be large enough to accommodate the minimum in the participation ratio. Heretofore, in the case of bending vibrations, the value of the vibron number N used to be fixed based only on the best fit to experiment.¹⁷

Another problem that can be tackled with the present formalism is the isomerization between the cis and trans geometric configuration of acetylene in the acetylene S_1 electronic state. The modeling in the algebraic framework of the bending degrees of freedom in a tetratomic molecule, which implies two coupled benders, requires a $U(3) \otimes U(3)$ dynamical algebra.^{21,59–61} An appropriate starting point would be the fit to the experimental bending vibrational term levels for each one of these two acetylene geometric configurations obtained making use of an algebraic Hamiltonian based on coupled dynamical algebra $U(3) \otimes U(3)$.⁶¹ The study of this case is of interest because this would be the first example of the identification of an ESQPT in experimental data for a system with more than one effective degree of freedom. In such

systems, the detection of the ESQPT precursors is expected to be more cumbersome than in the single degree of freedom cases.^{62,63}

Finally, it is interesting to note that the 2DVM eigenstates with a positive slope in the right end of Figure 1b have energies beyond the isomerization energy barrier. Thus, they cannot be unambiguously associated to one of the two molecular configurations and they correspond to the so-called bond-breaking states, which are often expressed with the $H_{0.5}CNH_{0.5}$ formula.⁴⁹ These eigenfunctions necessarily entangle both molecular configurations, something that in the 2DVM case was already noticed in ref 18 (see Figure 6 in this reference). A full description of the isomerizing HCN–HNC system at these energies requires the consideration of both molecules in a single system. This is a direction we plan to explore in the near future.

■ ASSOCIATED CONTENT

Supporting Information

The Supporting Information is available free of charge on the ACS Publications website at DOI: 10.1021/acs.jpca.9b07338.

Brief explanation of the classical limit of the 2DVM and of the effective frequency fitting procedure; results of the model for nonzero vibrational angular momentum; results obtained from the 2DVM fit to spectroscopically assigned ab initio energies including the comparison with experimental data (PDF)

■ AUTHOR INFORMATION

Corresponding Author

*E-mail: curropb@uhu.es. Phone: +34 959219789. Fax: +34 959219777.

ORCID

Francisco Pérez-Bernal: 0000-0002-3009-3696

Notes

The authors declare no competing financial interest.

■ ACKNOWLEDGMENTS

The authors thank José Miguel Arias, José Enrique García-Ramos, Franco Iachello, Georg Mellau, and Pedro Pérez Fernández for useful discussions and comments. J.K.-R. is grateful for the support from the Youth Employment Initiative and the Youth Guarantee program supported by the European Social Fund. L.F.S. is supported by the NFS Grant No. DMR-1603418. This study has been partially financed by the Consejería de Conocimiento, Investigación y Universidad, Junta de Andalucía and European Regional Development Fund (ERDF), ref SOMM17/6105/UGR and by the Centro de Estudios Avanzados de Física, Matemáticas y Computación (CEAFMC) of the Universidad de Huelva. Computer resources supporting this work were provided by the CEAFMC and Universidad de Huelva High Performance Computer (HPC@UHU) located in the Campus Universitario El Carmen and funded by FEDER/MINECO project UNHU-15CE-2848.

■ REFERENCES

- (1) Eyring, H. The activated complex in chemical reactions. *J. Chem. Phys.* **1935**, *3*, 107–115.
- (2) Wigner, E. The transition state method. *Trans. Faraday Soc.* **1938**, *34*, 29–41.

- (3) Baraban, J. H.; Changala, P. B.; Mellau, G. C.; Stanton, J. F.; Merer, A. J.; Field, R. W. Spectroscopic characterization of isomerization transition states. *Science* **2015**, *350*, 1338–1342.
- (4) Mellau, G. C.; Kyuberis, A. A.; Polyansky, O. L.; Zobov, N.; Field, R. W. Saddle point localization of molecular wavefunctions. *Sci. Rep.* **2016**, *6*, No. 33068.
- (5) Birge, R. T.; Sponer, H. The Heat of Dissociation of Non-Polar Molecules. *Phys. Rev.* **1926**, *28*, 259–283.
- (6) LeRoy, R. J.; Bernstein, R. B. Dissociation Energy and Long-Range Potential of Diatomic Molecules from Vibrational Spacings of Higher Levels. *J. Chem. Phys.* **1970**, *52*, 3869–3879.
- (7) Leroy, R. J.; Bernstein, R. B. Dissociation energies of diatomic molecules from vibrational spacings of higher levels: application to the halogens*. *Chem. Phys. Lett.* **1970**, *5*, 42–44.
- (8) Dixon, R. N. Higher vibrational levels of a bent triatomic molecule. *Trans. Faraday Soc.* **1964**, *60*, 1363–1368.
- (9) Child, M. S. Quantum states in a champagne bottle. *J. Phys. A: Math. Gen.* **1998**, *31*, 657–670.
- (10) Child, M. S.; Weston, T.; Tennyson, J. Quantum monodromy in the spectrum of H₂O and other systems: new insight into the level structure of quasi-linear molecules. *Mol. Phys.* **1999**, *96*, 371–379.
- (11) Child, M. S. *Adv. Chem. Phys.*; John Wiley & Sons, Ltd, 2008; Chapter 2, pp 39–94.
- (12) Harris, G. J.; Tennyson, J.; Kaminsky, B. M.; Pavlenko, Y. V.; Jones, H. R. A. Improved HCN/HNC linelist, model atmospheres and synthetic spectra for WZ Cas. *Mon. Not. R. Astron. Soc.* **2006**, *367*, 400–406.
- (13) Mellau, G. C. Complete experimental rovibrational eigenenergies of HNC up to 3743cm⁻¹ above the ground state. *J. Chem. Phys.* **2010**, *133*, No. 164303.
- (14) Mellau, G. C. Complete experimental rovibrational eigenenergies of HCN up to 6880 cm⁻¹ above the ground state. *J. Chem. Phys.* **2011**, *134*, No. 234303.
- (15) Baraban, J. H.; Matthews, D. A.; Stanton, J. F. Communication: An accurate calculation of the S1 C₂H₂ cis-trans isomerization barrier height. *J. Chem. Phys.* **2016**, *144*, No. 111102.
- (16) Winnewisser, M.; Winnewisser, B. P.; Medvedev, I. R.; Lucia, F. C. D.; Ross, S. C.; Bates, L. M. The hidden kernel of molecular quasi-linearity: Quantum monodromy. *J. Mol. Struct.* **2006**, *798*, 1–26.
- (17) Larese, D.; Iachello, F. A study of quantum phase transitions and quantum monodromy in the bending motion of non-rigid molecules. *J. Mol. Struct.* **2011**, *1006*, 611–628.
- (18) Larese, D.; Pérez-Bernal, F.; Iachello, F. Signatures of quantum phase transitions and excited state quantum phase transitions in the vibrational bending dynamics of triatomic molecules. *J. Mol. Struct.* **2013**, *1051*, 310–327.
- (19) Iachello, F. Algebraic methods for molecular rotation-vibration spectra. *Chem. Phys. Lett.* **1981**, *78*, 581–585.
- (20) Iachello, F.; Levine, R. D. *Algebraic Theory of Molecules*; Oxford University Press: Oxford, 1995.
- (21) Iachello, F.; Oss, S. Algebraic approach to molecular spectra: Two dimensional problems. *J. Chem. Phys.* **1996**, *104*, 6956–6963.
- (22) Iachello, F.; Pérez-Bernal, F.; Vaccaro, P. A novel algebraic scheme for describing nonrigid molecules. *Chem. Phys. Lett.* **2003**, *375*, 309–320.
- (23) Pérez-Bernal, F.; Santos, L.; Vaccaro, P.; Iachello, F. Spectroscopic signatures of nonrigidity: Algebraic analyses of infrared and Raman transitions in nonrigid species. *Chem. Phys. Lett.* **2005**, *414*, 398–404.
- (24) Gilmore, R.; Feng, D. Phase transitions in nuclear matter described by pseudospin Hamiltonians. *Nucl. Phys. A* **1978**, *301*, 189–204.
- (25) Gilmore, R. The classical limit of quantum nonspin systems. *J. Math. Phys.* **1979**, *20*, 891–893.
- (26) Pérez-Bernal, F.; Iachello, F. Algebraic approach to two-dimensional systems: Shape phase transitions, monodromy, and thermodynamic quantities. *Phys. Rev. A* **2008**, *77*, No. 032115.
- (27) Iachello, F. *Lie Algebras and Applications*; Springer: Heidelberg, 2015.
- (28) Iachello, F.; Arima, A. *The Interacting Boson Model*; Cambridge Press: Cambridge, 1987.
- (29) Iachello, F.; Zamfir, N. V. Quantum Phase Transitions in Mesoscopic Systems. *Phys. Rev. Lett.* **2004**, *92*, No. 212501.
- (30) Cejnar, P.; Jolie, J. Quantum phase transitions in the interacting boson model. *Prog. Part. Nucl. Phys.* **2009**, *62*, 210–256.
- (31) Cejnar, P.; Jolie, J.; Casten, R. F. Quantum phase transitions in the shapes of atomic nuclei. *Rev. Mod. Phys.* **2010**, *82*, 2155–2212.
- (32) Cejnar, P.; Macek, M.; Heinze, S.; Jolie, J.; Dobeš, J. Monodromy and excited-state quantum phase transitions in integrable systems: collective vibrations of nuclei. *J. Phys. A: Math. Gen.* **2006**, *39*, L515.
- (33) Caprio, M.; Cejnar, P.; Iachello, F. Excited state quantum phase transitions in many-body systems. *Ann. Phys.* **2008**, *323*, 1106–1135.
- (34) Winnewisser, B. P.; Winnewisser, M.; Medvedev, I. R.; Behnke, M.; De Lucia, F. C.; Ross, S. C.; Koput, J. Experimental confirmation of quantum monodromy: the millimeter wave spectrum of cyanogen isothiocyanate NCNCS. *Phys. Rev. Lett.* **2005**, *95*, No. 243002.
- (35) Zobov, N. F.; Shirin, S. V.; Polyansky, O. L.; Tennyson, J.; Coheur, P.-F.; Bernath, P. F.; Carleer, M.; Colin, R. Monodromy in the water molecule. *Chem. Phys. Lett.* **2005**, *414*, 193–197.
- (36) Dietz, B.; Iachello, F.; Miski-Oglu, M.; Pietralla, N.; Richter, A.; von Smekal, L.; Wambach, J. Lifshitz and excited-state quantum phase transitions in microwave Dirac billiards. *Phys. Rev. B* **2013**, *88*, No. 104101.
- (37) Zhao, L.; Jiang, J.; Tang, T.; Webb, M.; Liu, Y. Dynamics in spinor condensates tuned by a microwave dressing field. *Phys. Rev. A* **2014**, *89*, No. 023608.
- (38) Ginocchio, J. N.; Kirson, M. W. Relationship between the Bohr Collective Hamiltonian and the Interacting-Boson Model. *Phys. Rev. Lett.* **1980**, *44*, 1744–1747.
- (39) Dieperink, A. E. L.; Scholten, O.; Iachello, F. Classical Limit of the Interacting-Boson Model. *Phys. Rev. Lett.* **1980**, *44*, 1747–1750.
- (40) van Roosmalen, O.; Dieperink, A. Properties of a generalized pseudo-spin system: Application of the time dependent mean field method to and SU(4) invariant hamiltonian. *Ann. Phys.* **1982**, *139*, 198–211.
- (41) Sánchez-Castellanos, M.; Lemus, R.; Carvajal, M.; Pérez-Bernal, F. The potential energy surface of CO₂ from an algebraic approach. *Int. J. Quantum Chem.* **2012**, *112*, 3498–3507.
- (42) James, F.; Roos, M. MINUIT - System for function minimization and analysis of parameter errors and correlations. *Comput. Phys. Commun.* **1975**, *10*, 343–367.
- (43) Newville, M.; Stensitzki, T.; Allen, D. B.; Ingargiola, A. *LMFIT: Non-Linear Least-Square Minimization and Curve-Fitting for Python*; Astrophysics Source Code Library, 2014.
- (44) Lauvergnat, D.; Simon, A.; Maitre, P. Valence bond curve-crossing model of the 1,2-hydrogen shift in HCN and isovalent systems. *Chem. Phys. Lett.* **2001**, *350*, 345–350.
- (45) van Mourik, T.; Harris, G. J.; Polyansky, O. L.; Tennyson, J.; Császár, A. G.; Knowles, P. J. Ab initio global potential, dipole, adiabatic, and relativistic correction surfaces for the HCN–HNC system. *J. Chem. Phys.* **2001**, *115*, 3706–3718.
- (46) Makhnev, V. Y.; Kyuberis, A. A.; Zobov, N. F.; Lodi, L.; Tennyson, J.; Polyansky, O. L. High accuracy ab initio calculations of rotational–vibrational levels of the HCN/HNC system. *J. Phys. Chem. A* **2018**, *122*, 1326–1343.
- (47) Bačić, Z.; Light, J. C. Accurate localized and delocalized vibrational states of HCN/HNC. *J. Chem. Phys.* **1987**, *86*, 3065–3077.
- (48) Light, J. C.; Bacic, Z. Adiabatic approximation and nonadiabatic corrections in the discrete variable representation: Highly excited vibrational states of triatomic molecules. *J. Chem. Phys.* **1987**, *87*, 4008–4019.
- (49) Mellau, G. C. Rovibrational eigenenergy structure of the [H,C,N] molecular system. *J. Chem. Phys.* **2011**, *134*, No. 194302.
- (50) Santos, L. F.; Pérez-Bernal, F. Structure of eigenstates and quench dynamics at an excited-state quantum phase transition. *Phys. Rev. A* **2015**, *92*, No. 050101.

(51) Santos, L. F.; Távora, M.; Pérez-Bernal, F. Excited-state quantum phase transitions in many-body systems with infinite-range interaction: Localization, dynamics, and bifurcation. *Phys. Rev. A* **2016**, *94*, No. 012113.

(52) Pérez-Bernal, F.; Santos, L. F. Effects of excited state quantum phase transitions on system dynamics. *Progr. Phys. Fortschr. Phys.* **2017**, *65*, No. 1600035.

(53) Zelevinsky, V.; Brown, B. A.; Frazier, N.; Horoi, M. The nuclear shell model as a testing ground for many-body quantum chaos. *Phys. Rep.* **1996**, *276*, 85–176.

(54) Gubin, A.; Santos, F. L. Quantum chaos: An introduction via chains of interacting spins 1/2. *Am. J. Phys.* **2012**, *80*, 246–251.

(55) Heller, E. J. The correspondence principle and intramolecular dynamics. *Faraday Discuss. Chem. Soc.* **1983**, *75*, 141–153.

(56) Heller, E. J. Quantum localization and the rate of exploration of phase space. *Phys. Rev. A* **1987**, *35*, 1360–1370.

(57) Kloc, M.; Stránský, P.; Cejnar, P. Quantum quench dynamics in Dicke superradiance models. *Phys. Rev. A* **2018**, *98*, No. 013836.

(58) Pérez-Bernal, F.; Álvarez-Bajo, O. Anharmonicity effects in the bosonic U(2)-SO(3) excited-state quantum phase transition. *Phys. Rev. A* **2010**, *81*, No. 050101.

(59) Champion, J.-M.; Tamsamani, M. A.; Oss, S. Algebraic model of hindered rotations: application to H₂O₂. *Chem. Phys. Lett.* **1999**, *308*, 274–282.

(60) Iachello, F.; Pérez-Bernal, F. A Novel Algebraic Scheme for Describing Coupled Benders in Tetratomic Molecules. *J. Phys. Chem. A* **2009**, *113*, 13273–13286.

(61) Larese, D.; Caprio, M. A.; Pérez-Bernal, F.; Iachello, F. A study of the bending motion in tetratomic molecules by the algebraic operator expansion method. *J. Chem. Phys.* **2014**, *140*, No. 014304.

(62) Stránský, P.; Macek, M.; Cejnar, P. Excited-state quantum phase transitions in systems with two degrees of freedom: Level density, level dynamics, thermal properties. *Ann. Phys.* **2014**, *345*, 73–97.

(63) Stránský, P.; Macek, M.; Leviatan, A.; Cejnar, P. Excited-state quantum phase transitions in systems with two degrees of freedom: II. Finite-size effects. *Ann. Phys.* **2015**, *356*, 57–82.